THE JOURNAL OF BIOLOGICAL CHEMISTRY VOL. 290, NO. 23, pp. 14656–14667, June 5, 2015

Granulocyte/Macrophage Colony-stimulating Factor-dependent Dendritic Cells Restrain Lean Adipose Tissue Expansion*[S]

Received for publication, February 17, 2015, and in revised form, April 23, 2015 Published, JBC Papers in Press, April 30, 2015, DOI 10.1074/jbc.M115.645820

Nathalie Pamir[‡1], Ning-Chun Liu[‡], Angela Irwin[‡], Lev Becker[§], YuFeng Peng[¶], Graziella E. Ronsein[‡], Karin E. Bornfeldt[‡‖], Jeremy S. Duffield[**], and Jay W. Heinecke[‡]

From the Departments of [‡]Medicine, [¶]Rheumatology, and [‖]Pathology and the [**]Division of Nephrology and Lung Biology, University of Washington, Seattle, Washington 98109-8050 and the [§]Department of Pediatrics, University of Chicago, Chicago, Illinois 60637

Background: The role of myeloid cells in maintaining lean adipose tissue homeostasis is unclear.
Results: Adipose tissue dendritic cells suppress normal adipose tissue expansion by secreting fibronectin and matrix metalloproteinase 12.
Conclusion: Adipose tissue dendritic cells participate in maintaining normal adipose tissue homeostasis by preventing uncontrolled adipose tissue expansion.
Significance: Under normal physiology, dendritic cells participate in adipose tissue development.

The physiological roles of macrophages and dendritic cells (DCs) in lean white adipose tissue homeostasis have received little attention. Because DCs are generated from bone marrow progenitors in the presence of granulocyte/macrophage colony-stimulating factor (GM-CSF), we used GM-CSF-deficient (*Csf2*$^{-/-}$) mice fed a low fat diet to test the hypothesis that adipose tissue DCs regulate the development of adipose tissue. At 4 weeks of age, *Csf2*$^{-/-}$ mice had 75% fewer CD45^{+}Cd11b^{+} Cd11c^{+}MHCII^{+} F4/80^{-} DCs in white adipose tissue than did wild-type controls. Furthermore, the *Csf2*$^{-/-}$ mice showed a 30% increase in whole body adiposity, which persisted to adulthood. Adipocytes from *Csf2*$^{-/-}$ mice were 50% larger by volume and contained higher levels of adipogenesis gene transcripts, indicating enhanced adipocyte differentiation. In contrast, adipogenesis/adipocyte lipid accumulation was inhibited when preadipocytes were co-cultured with CD45^{+}Cd11b^{+}Cd11c^{+} MHCII^{+}F4/80^{-} DCs. Medium conditioned by DCs, but not by macrophages, also inhibited adipocyte lipid accumulation. Proteomic analysis revealed that matrix metalloproteinase 12 and fibronectin 1 were greatly enriched in the medium conditioned by DCs compared with that conditioned by macrophages. Silencing fibronectin or genetic deletion of matrix metalloproteinase 12 in DCs partially reversed the inhibition of adipocyte lipid accumulation. Our observations indicate that DCs residing in adipose tissue play a critical role in suppressing normal adipose tissue expansion.

In addition to adipocytes, white adipose tissue contains the stromal vascular fraction (SVF),[2] which includes vascular endothelial cells, fibroblasts, and several types of immune cells. Adipogenesis, the formation of new adipocytes from preadipocytes, is believed to be orchestrated by all of these cell types (1). However, adipogenesis must be closely regulated because both expansion (obesity) and shrinkage (lypodystrophy) associate with an array of metabolic consequences, such as diabetes, cardiovascular disease, and immunosuppression.

Adipogenesis is the continuous process of formation of new adipocytes from precursor cells responsible for maintaining a healthy adipose tissue. Impaired adipogenesis is associated with the pathogenesis of obesity-associated conditions, such as insulin resistance, hyperlipidemia, and type 2 diabetes (2–5). One of many factors controlling adipogenesis is Pref-1 (preadipocyte factor-1), which is highly expressed in preadipocytes and maintains these cells in an undifferentiated state during development (6). Pref-1 inhibits adipocyte differentiation through preventing down-regulation of SOX9 and the associated activation of SCD-1 (stearoyl-CoA desaturase-1) and FABP4 (fatty acid binding protein-4), leading to triacylglycerol accumulation (7, 8). In this study, we measured expression of Pref-1 and its downstream mediators as well as triacylglycerol accumulation to assess adipocyte differentiation and adipogenesis.

Non-lymphoid dendritic cells (DCs), a heterogeneous collection of cells derived from bone marrow, localize in most tissues in the steady state condition to help maintain tissue homeostasis (9, 10). Phenotypically, DCs express the hematopoietic marker CD45 and the integrin CD11c, and they constitutively express major histocompatibility complex class II (MHCII) (11).

DC maturation is stimulated by granulocyte/macrophage colony-stimulating factor (GM-CSF), which is produced by

* This work was supported, in whole or in part, by National Institutes of Health Grants HL092969, HL097365, HL062887, P30 DK035816, P30 DK017047, HL108897, and HL112625. This work was also supported in part by the Quantitative and Functional Proteomics Core of the Diabetes Research Center (University of Washington), the NORC Energy Balance and Glucose Metabolism Core, and American Heart Association Grant 11POST7390072.
[S] This article contains supplemental Table 1.
[1] To whom correspondence should be addressed: Oregon Health and Science University, 3181 S.W. Sam Jackson Park Rd. Portland, OR 97239-3011. E-mail: pamir@ohsu.edu.

[2] The abbreviations used are: SVF, stromal vascular fraction; DC, dendritic cell; BM-DC, bone marrow-derived DC; BM-DM, bone marrow-derived macrophage; TG, triacylglycerol; iNOS, inducible nitric-oxide synthase.

various cell types (12, 13). Consistently, *in vitro* GM-CSF prompts bone marrow cells to generate bone marrow-derived DCs (BM-DCs) (14, 15). GM-CSF-induced BM-DCs express CD11b, CD11c, and MHCII at higher levels than bone marrow-derived macrophages (BM-DMs; also found in white adipose tissue), both at the plasma membrane (16) and the mRNA level (17). Furthermore, mice lacking GM-CSF ($Csf2^{-/-}$ mice) have fewer $CD11c^+$ cells in their atherosclerotic plaques, indicating that GM-CSF modulates tissue levels of $CD11c^+$ cells *in vivo* (18).

In this study, we focus on the interaction between DCs and preadipocytes in adipose tissue and interrogate the involvement of GM-CSF-dependent DCs in adipose tissue homeostasis under steady state physiology.

Experimental Procedures

Mice—All studies were approved by the Animal Care and Use Committee of the University of Washington. Control ($Csf2^{+/+}$) and $Csf2^{-/-}$ mice (kind gift from Randy Seeley), both on a C57BL/6 background for more than 10 generations, were housed (3–5 mice/cage) in a specific pathogen-free barrier facility in a temperature-controlled room (22 °C) with a 12-h light/dark cycle and given free access to food and water. The mice were fed a low fat diet (Wayne Rodent BLOX 8604, Harlan Teklad Laboratory, Madison, WI) and were analyzed at 4, 15, and 25 weeks of age. Before necropsy, they were fasted for 4 h in the morning, bled from the retro-orbital sinus into tubes containing 1 mM EDTA, and killed by isofluorane inhalation. Tissues were collected and stored at −80 °C until analysis. Whole or remaining epididymal adipose depots were isolated and digested immediately for flow cytometry experiments.

Body Composition Analysis—The body fat content of immobilized male mice, 4 or 25 weeks of age, was determined by the Rodent Energy Metabolism and Body Composition Core (Nutrition Obesity Research Center, University of Washington). Adipose tissue mass was estimated by magnetic resonance spectroscopy (Echo Medical Systems, Houston, TX) from the area under the curve of the lipid peak at 200.1 MHz (19).

Insulin and Glucose Tolerance Testing—Insulin and glucose tolerance tests were performed after a 4-h fast. Mice were injected intraperitoneally with human insulin (1.0 unit/kg body weight; Lilly) or glucose (1 mg/g body weight) (20).

Body Composition, Food Intake, Locomotor Activity, and Indirect Calorimetry—Age- and sex-matched mice of each strain (5 mice/strain) were individually housed and acclimated to metabolic cages for 7 days. Food intake, physical activity, and calorimetric measurements were continuously recorded over a 24-h period during which food was available *ad libitum*.

Locomotor activity was assessed by the infrared beam break method, using an Opto-Varimetrix-3 sensor system, whereas food and water intake were measured with the Feed Scale System (Columbus Instruments, Columbus, OH). Rates of oxygen consumption (VO_2) and carbon dioxide production (VCO_2) were calculated, respectively, as the difference in air content between in-flow (room air) and out-flow (animals' expired air), with the known flow rate of ambient air. The rates were normalized to lean body mass (ml/kg lean mass/h). The respiratory quotient (RQ) was calculated as the ratio of CO_2 production (liters/min) over O_2 consumption (liters/min). Heat production (kcal/h) was presented as a surrogate for total energy expenditure; it was calculated using the standard Lusk formula (TEE (kcal/h) = $3.815 + 1.232 \times RQ) \times VO_2$ (liters/min)) (21, 22). Respirometric parameters for each mouse were measured for 2 min and recorded at 20-min intervals. After each batch of four mice, ambient air (used as reference air) was measured for 2 min.

Plasma Glucose, Insulin, and Lipid Measurements—Food was withheld from mice for 16 h before blood was collected from the retro-orbital plexus into tubes containing EDTA. Then fasting glucose levels were measured. At the time of sacrifice, blood was collected after a 4-h fast, and insulin, triglyceride, and cholesterol levels were determined, using an ultrasensitive insulin ELISA (Linco, Billerica, MA), L-type TG M assay (Wako Diagnostics), and Amplex Red cholesterol assay kit (Invitrogen).

Tissue Triacylglycerol (TG) and Glycogen Measurements—Equal portions of liver (0.3 mg) and the entire hind limb femoris muscles were homogenized in either water (glycogen) or phosphate-buffered saline (triglycerides). Glycogen was measured with a colorimetric glycogen assay kit (Abcam ab65620) per the manufacturer's guidelines. After lipid was extracted by the chloroform-free lipid extraction method (STA-612, Cell Biolabs, Inc.), total triglycerides were measured, using the same assay as for the plasma samples.

Adipose Tissue Fractionation—Under sterile conditions, adipose tissue was extracted and separated into stromal vascular cell and adipocyte fractions (23). Minced tissue in digestion buffer (Dulbecco's PBS supplemented by calcium and magnesium, Thermo Scientific) was incubated with 2 mg/ml type I collagenase (Worthington) for 45 min at 37 °C on an orbital shaker, filtered through 250-μm nylon mesh, and centrifuged at $500 \times g$ for 5 min. The pellet was resuspended in erythrocyte lysis buffer (Cell Signaling), incubated at room temperature for 5 min, and then filtered through a 70-μm nylon mesh and washed by centrifugation as above.

Quantitative Real-time PCR—Total RNA was extracted from frozen adipose tissue (100 mg), using acid-phenol reagent (Qiazol; Qiagen) and the RNeasy lipid tissue minikit (Qiagen, CA). All PCRs used SYBR Green, and mRNA was quantified using the $\Delta\Delta Ct$ method (24) with 18S and L32 ribosomal RNA as controls. The primers/probes were ordered from PrimerBank. An RT2-Profiler PCR array for mouse extracellular matrix and adhesion molecules (PAMM-013Z, Qiagen) was used to quantify relative mRNA levels in adipose tissue (25). Data were analyzed by software on the SABiosciences Web site.

Immunohistochemical and Morphometric Analyses—Adipose tissue was fixed in 10% buffered formalin overnight, dehydrated, and embedded in paraffin at 60 °C. The sections were counterstained with hematoxylin. Adipocyte area was determined from three high power (×200) fields/animal (7 mice/group), using a digital imaging system (ImagePro Plus, Media Cybernetics, Bethesda, MD).

Nuclei Counts—Two slides per mouse ($n = 3$ mice/genotype) were scanned in bright field at ×20 magnification, using the Hamamatsu NanoZoomer Digital Pathology System. The digital images were then imported into Visiopharm software for

quantitative analysis. Using the Visiopharm image analysis module, regions of interest were manually detected and sampled at 100% around the adipose tissue. The areas around vessels were manually excluded. The software converted the initial digital imaging into grayscale values, using two features, RGB-B and IHS-S. Visiopharm was then trained to label nuclei and adipose tissue, using a configuration based on a threshold of pixel values. Using this configuration, we processed images in batch mode to generate the desired outputs. All studies were performed by an observer blinded to animal genotype.

BM-DMs and BM-DCs—Bone marrow harvested from femurs and tibias of 16-week-old mice was gently suspended in RPMI. Cells were collected by centrifugation (300 × *g*, 5 min), plated (2×10^6) in 6-well plates, and cultured for 7 days in RPMI supplemented with 10% FBS, 1% penicillin, and either 30 ng/ml mouse recombinant M-CSF or 10 ng/ml GM-CSF (R&D Systems, Minneapolis, MN). Medium was replaced on days 4 and 6. Conditioned medium was prepared by overnight incubation with serum-free medium and was concentrated 20 times by centrifugation (300 × *g*, 20 min) with centrifugal filter units (Amicon Ultra 3K, Millipore). Protein concentration was measured by the BCA protein assay (Pierce), and the medium was than rediluted with fresh medium to obtain 1× concentration. RNA was harvested from cells, using the RNeasy mini kit (Qiagen) (14, 15).

Flow Cytometry and Cell Sorting—After isolation of SVF from the epididymal fat pads, the SVF pellet was incubated with an Fc receptor blocker (CD16/32) and a mixture of monoclonal antibodies. Propidium iodide was used to eliminate dead cells from the analysis. A list of antibodies used is provided in supplemental Table 2. Cells were sorted on a FACSCanto II cell analyzer, and the leukocyte population was identified on side scatter *versus* forward scatter plots followed by a propidium iodide (PI^-) and $CD45^+$ selection (26). A dump gate for CD80, CD86, CD103, CD4, CD8, and DEC205 under FITC was used to verify that $Cd45^+Cd11b^+Cd11c^+MHCII^+$ do not express any of these proteins included.

Antigen Presentation Assay—Relevant cell populations isolated from 10 mice were pooled and seeded into a 96-well plate, at least in duplicate, at 7,500 cells/well. Following overnight incubation, the cells were exposed to ovalbumin (200 μg/ml) overnight and incubated for 4 days with 10^5 ovalbumin-specific T cell receptor transgenic (OT-I) cells labeled with cell tracer, proliferation marker, carboxyfluorescein diacetate, and succinimidyl ester. T cell proliferation was assessed by loss of intensity of succinimidyl ester of the CD44- (activation marker) and CD8-positive cells (27).

Antibodies—Antibodies were purchased from eBioscience: Cd45 (48-0451), Cd11b (25-0112), Cd11c (12-0114), F4/80 (11-24801), MHCII (11-5980), Cd80 (11-0801), Cd86 (11-0862), Cd205 (17-2051), Cd4 (11-0041), Cd8 (11-0083), Cd44 (48-0441), PI (00-6990), Fcblock (14-0161).

Culture of 3T3-L1 Cells—3T3-L1 cells (ATCC, Manassas, VA) were cultured in DMEM with 10% calf serum and 1% penicillin-streptomycin in the required plate format. For 96-well plates, the cells were seeded at 10,000/well. For 24-well plates, they were seeded at 25,000 cells/well. Following overnight culture, the medium was supplemented with 1 μM dexamethasone, 0.25 μM isobutylmethylxanthine, and 2 μM insulin for the first 3 days and 2 μM insulin for the remaining 2 days. Differentiation was assessed by measuring TG accumulation at day 5, using AdipoRed adipogenesis assay reagent (Lonza). Oil Red O staining was used to image neutral lipid accumulation in the cells. Briefly, formalin-fixed cells were washed with 60% isopropyl alcohol, stained with oil red O for 10 min, and then washed extensively with water prior to imaging (28).

Statistical Analyses—Data represent means ± S.E. Unpaired two-tailed Student's *t* test and one-way analysis of variance followed by Tukey correction were used for statistical analysis. $p < 0.05$ was considered significant.

Results

GM-CSF Induces Increased Fat Mass in Young Mice, and the Effect Is Maintained throughout Adulthood—Two previous studies showed that adult $Csf2^{-/-}$ mice have either normal body weight when fed a low fat diet or increased body weight when fed a high fat diet compared with wild-type littermate controls (29, 30). However, both reports failed to report adiposity. We were interested in the possibility that GM-CSF could also help to regulate normal adipogenesis and adipose tissue expansion from a young age. To study its contribution to adipose tissue expansion in young mice, we fed 3–4-week-old mice a low fat diet and assessed their adiposity. Young $Csf2^{-/-}$ mice showed a significant 20% increase in adiposity, whereas their body weights and lean mass were comparable with those of wild-type mice (Fig. 1, *A*, *C*, and *E*). We next evaluated adiposity in low fat-fed adult $Csf2^{-/-}$ mice at 15 and 25 weeks of age. Data from both time points yielded similar results (data not shown). The differences at 25 weeks of age are shown in Fig. 1. Body weight and lean mass of the adult $Csf2^{-/-}$ mice were 12% lower than those of the wild-type mice. However, fat pad weight, as a percentage of total body weight, was 2.5 times higher (Fig. 1, *B*, *D*, and *F*), which was consistent with the results from the 3–4-week-old mice.

Increased adiposity is characterized by larger adipocytes that accumulate more triglyceride and/or by increased adipocyte number. We confirmed that adiposity was greater by quantifying the mean adipocyte area in hematoxylin-stained sections. The adipocyte area was 50% larger in the $Csf2^{-/-}$ mice than in the wild-type controls (Fig. 1, *G* and *H*). The strains had comparable numbers of nuclei per adipose-only tissue area (0.0019 ± 0.0000025 *versus* 0.0016 ± 0.00011 nuclei/μm^2, $n = 3$, $p = 0.20$ in $Csf2^{+/+}$ *versus* $Csf2^{-/-}$ mice, respectively). However, the $Csf2^{-/-}$ mice had 50% more adipose tissue weight than the control mice (Fig. 1*F*). It is therefore possible that mice lacking GM-CSF harbor more adipocytes per adipose depot. Overall, these findings demonstrate that, despite modestly reduced body weight, GM-CSF deficiency results in a robust increase in body fat content that is manifested as early as 3–4 weeks of age and is maintained through adulthood. It is possible that the main effect of GM-CSF is on adipose tissue hypertrophy, with a smaller contribution to adipogenesis.

$Csf2^{-/-}$ *Mice Exhibit Favorable Glucose Homeostasis*—To assess whether increased adiposity had a metabolic impact, we also measured fasting plasma glucose, triglycerides, total cholesterol levels, liver triacylglycerides and glycogen, and muscle

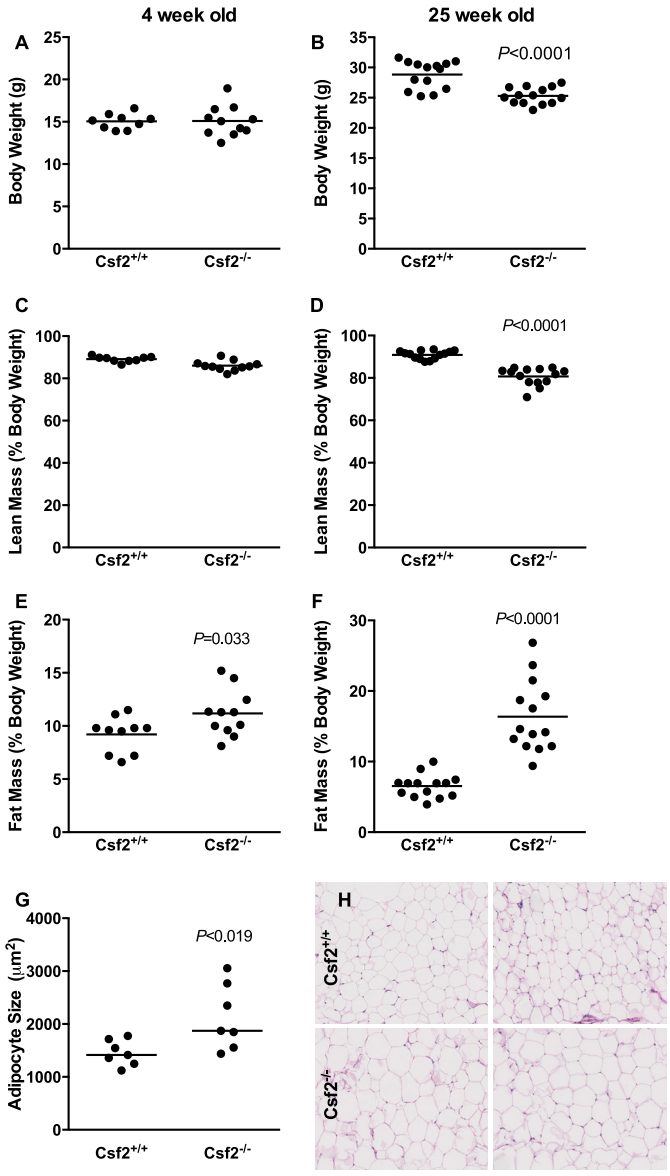

FIGURE 1. **Csf2$^{-/-}$ mice exhibit increased adiposity when fed a low fat diet.** *A* and *B*, body weight. Body composition is presented as lean mass (*C* and *D*) and fat mass (*E* and *F*) normalized to body weight. Adipose tissue morphology mean adipocyte area (*G*) and images showing the morphology of the adipose tissue by H&E staining (*H*).

triacylglycerides and glycogen in lean adult mice (Table 1). Despite increased adiposity, the fasting glucose levels of the adult *Csf2*$^{-/-}$ mice were more favorable than those of the control mice. Furthermore, plasma triglyceride levels were elevated although liver and skeletal muscle TG and glycogen levels remained unchanged.

In rodents and humans, increased adiposity and larger adipocytes are usually associated with a decline in peripheral insulin sensitivity (31, 32). However, the adult *Csf2*$^{-/-}$ mice, despite increased adiposity, had greater glucose tolerance and insulin sensitivity (Fig. 2, *A* and *B*) in response to glucose tolerance and insulin sensitivity tests. Consistently, the *Csf2*$^{-/-}$ mice required less insulin to maintain blood glucose levels than the wild-type mice, as shown by the 50% reduction in plasma insulin levels (Fig. 2*C*). Short term and overnight fasting plasma

TABLE 1
Plasma and tissue parameters for *Csf2*$^{+/+}$ and *Csf2*$^{-/-}$ mice
Triglycerol and total cholesterol were measured following a 4-h fast.

Parameters	Csf2$^{+/+}$	Csf2$^{-/-}$	*p* value
4-h fasting glucose (mg/dl)	120.8 ± 6.6	90.6 ± 13.8	<0.0001
Overnight fasting glucose (mg/dl)	148.7 ± 41.8	102.5 ± 30.4	<0.0001
TG (mg/dl)	36.1 ± 13.5	65.2 ± 18.2	0.0002
Total cholesterol (mg/dl)	119.5 ± 51.1	129.6 ± 18.2	0.52
Liver TG (μg/mg protein/g tissue weight)	15.57 ± 13.87	18.81 ± 6.22	0.64
Muscle TG (μg/mg protein/g tissue weight)	13.81 ± 7.53	12.27 ± 5.18	0.71
Liver glycogen (μg/mg protein/g tissue weight)	0.154 ± 0.079	0.215 ± 0.023	0.48
Muscle glycogen (μg/mg protein/g tissue weight)	0.411 ± 0.058	0.81 ± 0.25	0.16

glucose levels were also reduced in the *Csf2*$^{-/-}$ mice, confirming better glucose homeostasis than in the wild-type controls (Table 1).

Csf2$^{-/-}$ *Mice Exhibit Increased Energy Expenditure*—To understand the contribution of DCs to energy metabolism, we measured food intake, ambulatory activity (Fig. 2*D*), heat production (Fig. 2*F*), and oxygen consumption (Fig. 2*E*). *Csf2*$^{-/-}$ mice ate significantly more during the light cycle (1.14 ± 0.10 *versus* 2.11 ± 0.25 g; $n = 5$, $p = 0.0071$, *Csf2*$^{+/+}$ *versus Csf2*$^{-/-}$, respectively). However, the groups had comparable 24-h cumulative food intake. Compared with the *Csf2*$^{+/+}$ mice, dark cycle ambulatory activity was 50% lower for the *Csf2*$^{-/-}$ mice (Fig. 2*D*). Both oxygen consumption (Fig. 2*E*) and heat production (Fig. 2*F*) increased by ~15% during the light cycle and also over 24 h in the *Csf2*$^{-/-}$ mice, suggesting increased metabolic rate. Meanwhile, the strains had comparable respiratory quotients in both the light and dark cycles, suggesting similar basal metabolic rates. Overall, when compared with the *Csf2*$^{+/+}$ mice, the *Csf2*$^{-/-}$ mice ingested a comparable number of calories over the 24-h cycle but had higher energy expenditure. These observations are discordant with the increased body adiposity of the *Csf2*$^{-/-}$ mice. This suggests that mechanisms other than energy expenditure contribute to the increased adiposity observed in *Csf2*$^{-/-}$ mice.

Adipose Tissue of Csf2$^{-/-}$ *Mice Contains Fewer GM-CSF-dependent DCs*—GM-CSF is required for the maturation of non-lymphoid DCs *in vivo* (33). *In vitro*, GM-CSF treatment consistently promotes the differentiation of bone marrow progenitor cells into immature BM-DCs, and this system serves as a model for generating monocyte-derived DCs that share several characteristics with their *in vivo* DC counterparts (14, 15). Specifically, BM-DCs produce TNF and iNOS and exhibit higher levels of the cell surface markers CD11c and MHCII and lower levels of F4/80, as compared with BM-DMs (16).

To examine the effect of GM-CSF deprivation on myeloid cell populations in adipose tissue, we assessed myeloid cell populations in isolated SVF. Four-week-old *Csf2*$^{-/-}$ mice had a profound reduction in their CD45$^+$CD11b$^+$CD11c$^+$ cell population compared with their wild-type littermates: 4.8% *versus* 18.7% as a percentage of CD45$^+$ cells (Fig. 3*A*). Furthermore, this B$^+$C$^+$ cell population was F4/80-negative and MHCII-positive (Fig. 3, *B* and *C*). Consistently, SVF from adult *Csf2*$^{-/-}$ mice had lower Cd11b and Cd11c gene expression (Fig. 3*I*). For example, adipose tissue from adult 25-week-old *Csf2*$^{-/-}$ mice

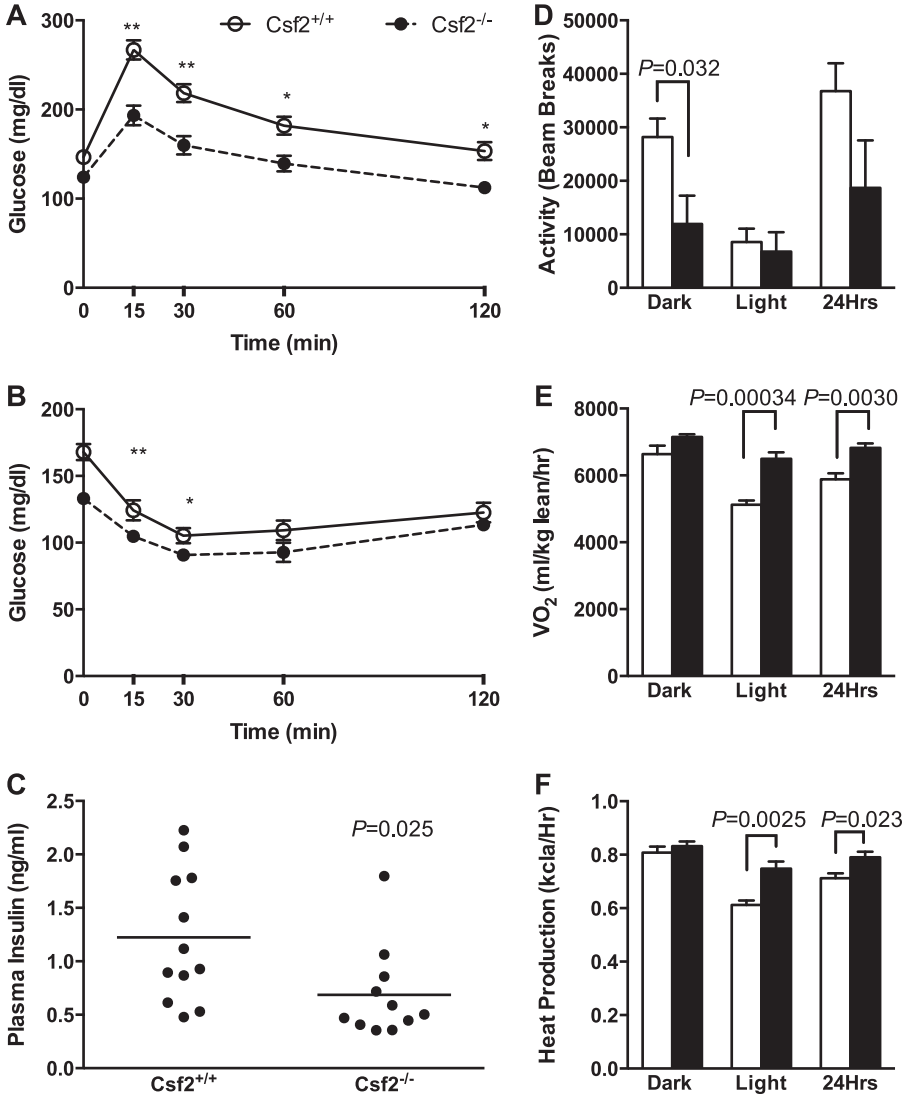

FIGURE 2. **Characterization of glucose metabolism and energy homeostasis.** Glucose tolerance (*A*) and insulin tolerance (*B*) tests were performed with adult male mice ($n = 12–17$; *, $p < 0.01$; **, $p < 0.001$). Plasma insulin levels were measured following a 4-h fast (*C*). Energy homeostasis was assessed by indirect calorimetry for five adult male mice. Ambulatory activity (*D*), oxygen consumption VO_2 (*E*), and heat production (*F*) are shown.

showed a decrease in $CD45^+CD11b^-CD11c^+$ (B^-C^+) and $CD45^+Cd11b^+Cd11c^+$ (B^+C^+) leukocyte subpopulations (Fig. 2, *D*, *G*, and *H*). Both subpopulations expressed low levels of F4/80; however, the $CD45^+Cd11b^+Cd11c^+$ B^+C^+ but not $CD45^+CD11b^-CD11c^+$ (B^-C^+) population expressed high levels of MHCII (Fig. 3, *E* and *F*). Furthermore, these cells did not express several lymphocyte and plasmacytoid DC markers, including CD4, CD8, CD103, DEC 205, CD80, and CD86 (data not shown), indicating that the $CD45^+CD11b^-CD11c^+$ (B^-C^+) and $CD45^+Cd11b^+Cd11c^+$ (B^+C^+) cells were not lymphocytes, plasmacytoid DCs, skin DCs, or mature DCs. CD11c and MHCII are abundantly present on the DC surface (16, 34). Under physiological conditions, 20% of all myeloid cells in adipose tissue are GM-CSF-dependent DCs.

MHCII plays an important role in antigen presentation, a major function of DCs (11, 35, 36). Once mature, DCs contribute to antigen presentation and T cell priming (37) and activation (35).

To test the antigen-presenting capabilities of $CD45^+Cd11b^+Cd11c^+$ B^+C^+ and $CD45^+Cd11b^-Cd11c^+$ B^-C^+ cells isolated from adipose tissue, we compared those cell populations with BM-DCs generated *in vitro*. Only the $CD45^+Cd11b^+Cd11c^+$ B^+C^+ subpopulation was functionally comparable with GM-CSF-dependent BM-DCs generated *in vitro* (Fig. 3*J*).

In summary, $Csf2^{-/-}$ mice exhibit increased adiposity, and their adipose tissue has a dramatically reduced $CD45^+CD11b^+$ $CD11c^+MHCII^+F480^-$ DC population from an early age and throughout adulthood. These observations suggest that DCs derived from GM-CSF-dependent monocytes play a critical role in restricting adipose tissue homeostasis and development.

The Membrane Proteome and Secretome of Myeloid Cells Derived from M-CSF- and GM-CSF-stimulated Bone Marrow Display Wide Polarity—To evaluate the possibility that adipose tissue DCs secrete factors that inhibit adipose tissue expansion, we first performed gene expression and mass spectrometric analyses of cell surface proteins and proteins secreted from (*a*) BM-DMs differentiated *in vitro* by M-CSF (macrophage colony-stimulating factor) and (*b*) BM-DCs differentiated *in vitro* by GM-CSF. The gene expression panel (Fig. 4*A*) demonstrated that BM-DCs express several genes, including *Arg 1*, *Cd11c*,

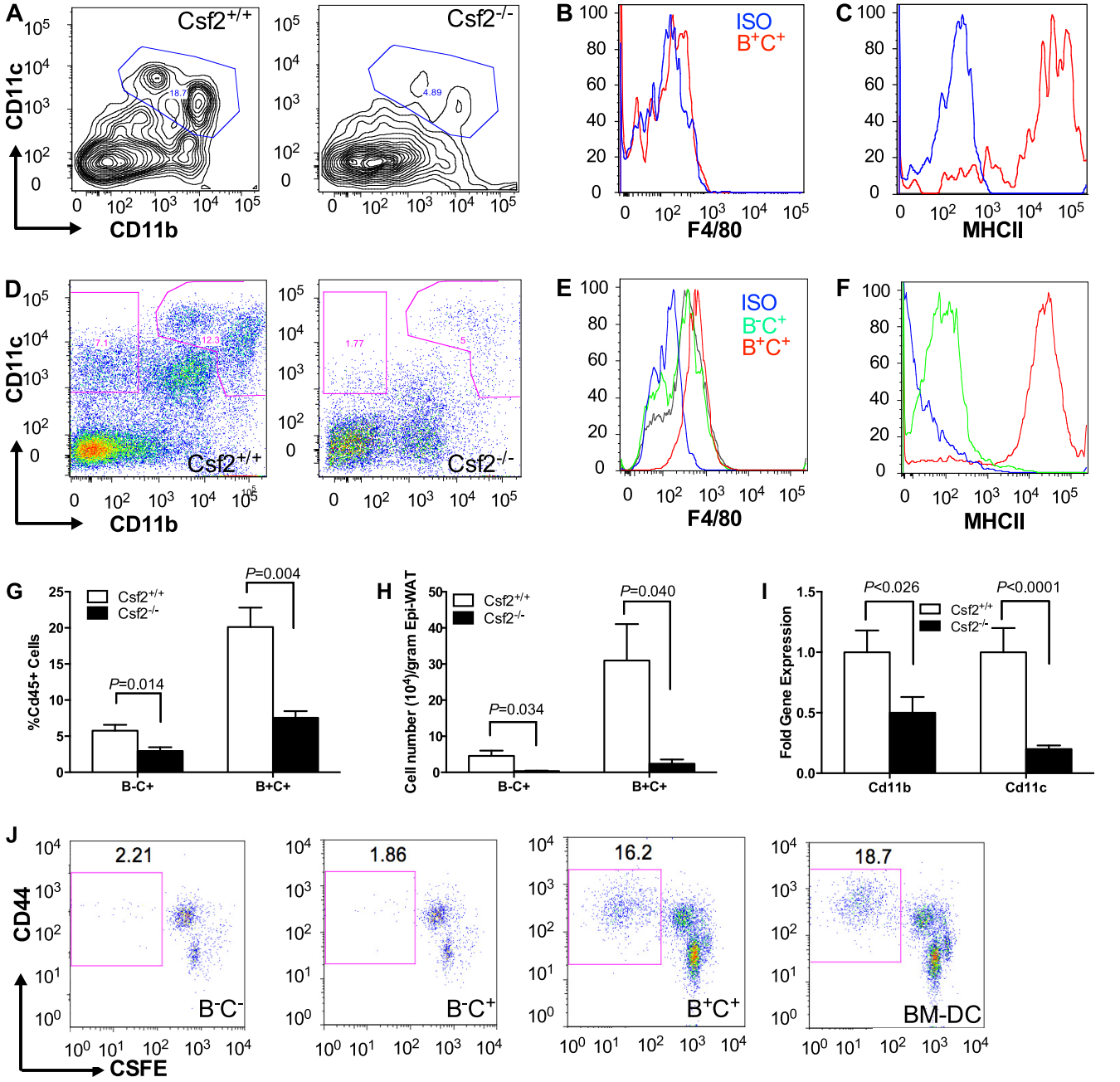

FIGURE 3. **Characterization of adipose tissue myeloid populations by surface markers, gene expression, and antigen presentation.** Representative FACS plots showing CD11b- and CD11c-expressing CD45$^+$ cells and subpopulations in 4-week-old mice (*A*, pooled from 10 mice) and 25-week-old mice (*D*, n = 12). F4/80 and MHCII expression by CD45+CD11b-CD11c+ (B^-C^+) and CD45$^+$CD11b$^+$CD11c$^+$ (B^+C^+) subpopulations was measured in 4-week-old mice (*B* and *C*) and 25-week-old mice (*E* and *F*). The myeloid subpopulations were quantified for 25-week-old mice as a percentage of CD45$^+$ cells (*G*) and per g of adipose tissue (*H*). CD11b and CD11c gene expression in the SVF of epididymal adipose depot was quantified for 25-week-old mice (*I*, n = 12). A T cell proliferation assay was performed to assess the antigen presentation capability of B^-C^+ and B^+C^+ myeloid subpopulations (*J*). Myeloid subpopulations were isolated from pooled SVF from 10 adult wild-type mice.

Ym1, and *iNOS* (*Nos2*), at higher levels than BM-DMs. The relative increase in iNOS expression in BM-DCs is consistent with recent characterization of the DC cell surface proteome (16). Thus, *Nos2* gene expression is 4-fold higher in BM-DCs than in BM-DMs (Fig. 4*A*). It is 70% lower in SVF from *Csf2*$^{-/-}$ mice than in SVF from controls (Fig. 4*C*). Consistently, *Nos2* gene expression is arbitrarily increased 100-fold in CD45$^+$ CD11b$^+$Cd11c$^-$ B^+C^+ cells (the BM-DC *in vivo* counterparts) compared with CD45$^+$CD11b$^-$Cd11c$^-$ B^-C^- cells, which do not express detectable *Nos2* (34–36 cycle number) (Fig. 4*E*). Because IL-12β is a marker for DC maturation (38), it was 2-fold higher in the BM-DCs and 30-fold higher in the CD45$^+$CD11b$^+$Cd11c$^+$ cells than in the CD45$^+$CD11b$^+$ Cd11c$^-$ population (Fig. 3, *A* and *D*). Conversely, levels of *Il10* (Fig. 4*E*) and *Tnfa* (Fig. 4*G*) gene transcripts in the CD45$^+$CD11b$^+$Cd11c$^+$ and CD45$^+$CD11b$^+$Cd11c$^-$ B^+C^+ subpopulations were comparable, although transcript levels of both genes were significantly higher in the BM-DCs than in the BM-DMs (Fig. 4*A*). Furthermore, the BM-DCs also secreted large amounts of matrix metalloproteinase (MMP12) and

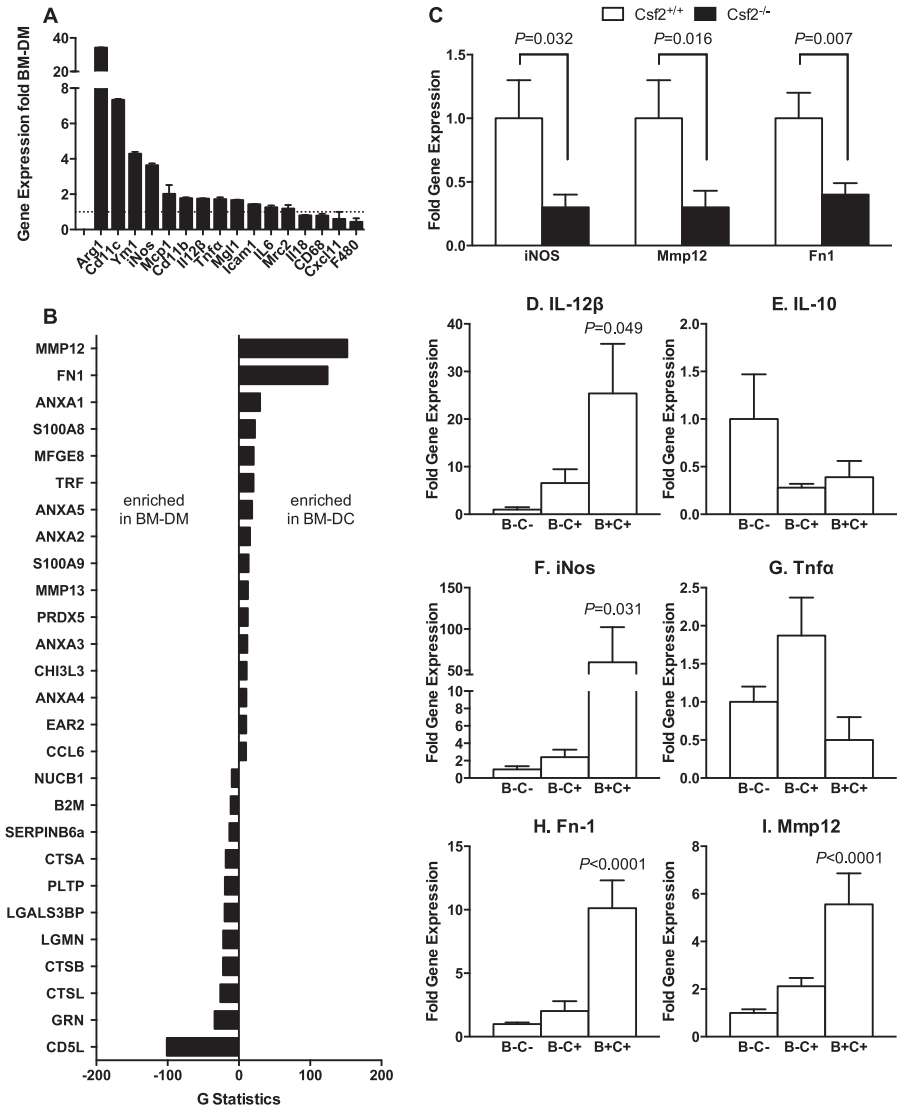

FIGURE 4. **Characterization and comparison of BM-DCs and *in vivo* CD45$^+$CD11b$^+$CD11c$^+$ counterparts.** *A*, gene expression profile of expressed normalized BM-DM. *Dotted line*, BM-DMs; *black bars*, BM-DCs differentiated *in vitro* (from 6 sets of experiments). *B*, secreted proteome determined by proteomic analysis of conditioned medium from BM-DMs and BM-DCs ($n = 6$). *C*, DC-specific gene expression in SVF ($n = 6$). *D–H*, gene expression profiles for the isolated myeloid cell populations generated *in vivo* ($n = 12$).

fibronectin (Fn1) (Fig. 4*B*). The full spectrum of secreted proteins is presented in supplemental Table 1. SVF from *Csf2*$^{-/-}$ mice had 2-fold lower transcript levels for *Fn1* and *Mmp12* (Fig. 4*C*), whereas CD45$^+$CD11b$^+$Cd11c$^+$ B$^+$C$^+$ cells had 5-fold higher *Mmp12* gene expression (Fig. 4*I*) and 10-fold higher *Fn1* (Fig. 4*H*) gene expression than the CD45$^+$CD11b$^+$Cd11c$^-$ B$^-$C$^-$ population. These results support the conclusion that the CD45$^+$CD11b$^+$Cd11c$^+$ DCs isolated from adipose tissue are comparable in their cell surface markers with the GM-CSF-dependent BM-DCs generated *in vitro* (Cd45, CD11b, CD11c, MHCII, F4/80), secreted proteins (MMP12 and FN1), and gene expression (*Nos2* and *IL12b*). They also appear to be functionally comparable when assessed by antigen presentation (Fig. 4*J*).

DC-conditioned Medium Inhibits Adipocyte Differentiation in Vitro—We next treated differentiating preadipocytes (3T3-L1 cells) with different concentrations of conditioned medium from BM-DMs or BM-DCs that had differentiated *in vitro*. Although conditioned medium from BM-DMs had no effect on preadipocyte differentiation, BM-DC-conditioned medium dramatically inhibited preadipocyte differentiation and lipogenesis (measured as adipocyte neutral lipid accumulation) in a concentration- dependent manner (Fig. 5, *A* and *B*). At 50 μg/ml, BM-DC-conditioned medium also modified several genes involved in adipogenesis and lipid accumulation. Thus, *Pparγ*, *Cebpα*, *Cebpδ*, *Cebpγ*, *Scd1*, and *Fabp4* were significantly down-regulated, and the preadipocyte factor 1 (*Dlk1* or *Pref-1*) was significantly up-regulated (6-fold) when compared with cells treated with BM-DM-conditioned medium at the same concentration (Fig. 5*D*). Pref-1 is secreted from preadipocytes and inhibits adipocyte differentiation (39). We therefore showed that exposure to BM-DC-conditioned medium impairs preadipocyte to adipocyte differentiation.

Importantly, recombinant GM-CSF had no effect on adipocyte differentiation, confirming that factors secreted from DCs, rather than GM-CSF itself, is responsible for the inhibitory effect we observed (Fig. 5*C*). Thus, the increased adiposity

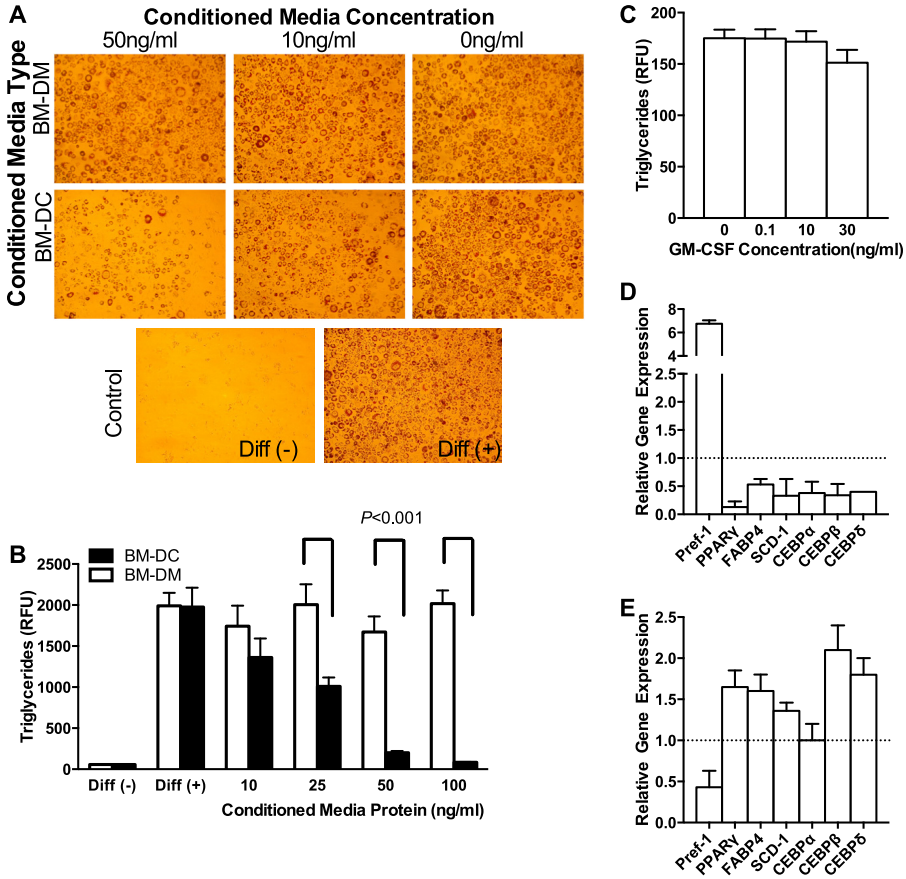

FIGURE 5. **Inhibition of adipocyte differentiation by BM-DCs.** *A*, visualization of inhibition of adipocyte differentiation. *B*, quantification of dose-dependent inhibition of adipocyte differentiation. *C*, quantification of adipocyte differentiation after GM-CSF treatment (mean of 4 experiments is presented). *D*, adipogenesis gene expression profile for preadipocytes treated with BM-DM-conditioned medium (*dotted line*) and BM-DC-conditioned medium (*white bars*). *E*, adipogenesis gene expression profile in epididymal fat pad of wild-type (*dotted line*) and Csf2$^{-/-}$ mice ($n = 12$).

and enlargement of adipocytes that we found in the *Csf2*$^{-/-}$ mice was associated with significantly increased expression of genes involved in adipogenesis and a 2-fold reduction in *Pref-1* levels in the adipose tissue (Fig. 5*E*). These observations suggest that, under physiological conditions, DCs limit adipocyte differentiation by their secreted products and that the reduction in adipose tissue DCs allows increased adiposity.

Mice deficient in GM-CSF display alterations in their vascular extracellular matrix (40). Increased adipocyte differentiation and enlarged adipocytes might alter adipose tissue extracellular composition. We tested that hypothesis by measuring levels of extracellular matrix gene transcripts in whole adipose tissue from wild-type and Csf2$^{-/-}$ mice, using a superarray. We concluded that the extracellular matrix was altered because levels of several extracellular matrix genes (*Col2a1*, *Entpd1*, *Hc*, *Lamc1*, *Sparc*, *Timp2*, *Vcam1*) were modified in a statistically significant manner (Table 2).

MMP12 and Fn1 Are Mediators of DC-dependent Inhibition of Adipogenesis—Our observation that medium conditioned by BM-DCs inhibits adipogenesis in a concentration-dependent manner suggests that factors secreted from DCs are responsible. As shown by the secretome proteomics (Fig. 4*B*), MMP12 and FN1 are abundantly secreted proteins from BM-DCs. Moreover, gene expression of *Mmp12* and *Fn1* is significantly up-regulated in CD45^{+}CD11b^{+}Cd11c^{+} B^{+}C^{+} cells (3- and 5-fold, respectively) compared with CD45^{+}CD11b^{+}Cd11c^{-} B^{-}C^{+} cells (Fig. 4, *H* and *I*). Fibronectin has been shown to inhibit adipocyte differentiation (41) by interacting with Pref-1 (8).

To determine whether MMP12 secreted by DCs affects adipocyte differentiation, we used bone marrow from *Mmp12*$^{-/-}$ mice. Lack of MMP12 significantly improved adipogenesis by 30% (Fig. 6*A*). To explore the role of Fn-1, we silenced Fn-1 gene expression in BM-DCs and determined how the resulting conditioned medium affected adipogenesis. Lack of Fn-1 significantly improved adipocyte differentiation and triglyceride accumulation by 20% (Fig. 6*B*). Taken together, our results suggest that the MMP12 and fibronectin proteins secreted from DCs contribute to inhibition of adipocyte differentiation.

The secretome of BM-DCs is also enriched in S100A8 and S100A9, two calcium-binding proteins in the S100 family (Fig. 4*B*). We assessed the role of secreted S100A8 and S100A9 on adipocyte differentiation, using *S100a9*$^{-/-}$ mice that were also deficient in S100A8 protein (42). Lack of S100A8 and S100A9 improved adipogenesis by 30% at 50 ng/ml concentration measured by triglyceride accumulation (163.55 ± 9.870 and 272.5 ± 4.010, $n = 4$, $p < 0.0001$ for wild-type *versus* *S100a9*$^{-/-}$ dendritic cells).

However, levels of S100A8 and S100A9 did not appear to be low in the SVF fraction of adipose tissue from the *Csf2*$^{-/-}$ mice (data not shown). Furthermore, *S100a9*$^{-/-}$ mice do not exhibit increased adiposity (42). Hence, it is not clear whether S100A8

TABLE 2

Differentially expressed extracellular matrix and adhesion molecule genes in adipose tissue

Gene transcripts were measured by an extracellular matrix superarray in epididymal adipose tissue from six $Csf2^{+/+}$ and $Csf2^{-/-}$ mice. CI, confidence interval.

Gene	Change from control	95% CI	*p* value
	-fold		
Col2a1	2.1314	(0.97, 3.30)	0.043576
Entpd1	1.4685	(1.07, 1.86)	0.034928
Hc	2.6183	(0.67, 4.56)	0.021171
Lamc1	4.0793	(1.53, 6.63)	0.001754
SIparc	0.6997	(0.49, 0.90)	0.026548
Timp2	3.1314	(0.83, 5.43)	0.018904
Vcam1	2.1279	(1.24, 3.02)	0.009766

and S100A9 secreted by DCs also help to inhibit adipocyte differentiation.

DCs from Adipose Tissue Inhibit Adipocyte Differentiation—To confirm our *in vitro* findings, we isolated $CD45^+CD11b^+Cd11c^+$ B^+C^+ cells from adipose tissue of 10 wild-type mice and co-cultured those cells with preadipocytes in the presence of differentiation medium. The presence of $CD45^+CD11b^+Cd11c^+$ cells inhibited adipocyte differentiation, whereas $CD45^+CD11b^-Cd11c^-$ and $CD45^+CD11b^+Cd11c^-$ cells had no effect, as measured by triglyceride accumulation (Fig. 6*C*) and gene expression (Fig. 6, *D–F*). Pref-1 was 2-fold higher, whereas *PPARg* and *Fabp4* were down-regulated. We repeated these experiments twice and therefore did not calculate statistical significance. Thus, $CD45^+CD11b^+Cd11c^+$ DCs isolated from adipose tissue inhibit both adipogenesis and triacylglycerol accumulation.

Discussion

Increased Adiposity in $Csf2^{-/-}$ Mice Is Not Explained by Changes in Energy Homeostasis, but It Might Promote Insulin Sensitivity—Adipose tissue contains most of the energy stores in healthy mammals (2). These stores participate in energy homeostasis by regulating both food intake and energy expenditure (43). Despite increased energy expenditure (measured as VO_2 consumption and heat production) and comparable food intake, the mice lacking GM-CSF-dependent DCs had increased adipose tissue mass. This observation strongly suggests that DCs participate locally in regulating adipose tissue physiology. Conversely, $Csf2^{-/-}$ mice exhibited no differences in skeletal muscle or liver TG or glycogen levels, indicating that adipose tissue does not expand at the expense of substrate availability in other tissues targeted by insulin. Although an effect of *Csf2* on other tissues cannot be ruled out, our results strongly suggest that DCs limit adipose tissue expansion. The effects of adipose tissue DCs on plasma triglyceride levels, adipocyte metabolism, and fatty acid oxidation warrant further investigation.

Lean $Csf2^{-/-}$ mice fed a low fat diet showed a 2-fold increase in percentage of fat mass while maintaining comparable body weight. They also had favorable glucose profiles in response to glucose and insulin challenges. These findings support the adipose tissue expandability hypothesis, which states that the adipose tissue's capacity to expand, determined by both genetic and environmental factors, prevents lipid overspill and protects against peripheral insulin resistance (44). It is important to note

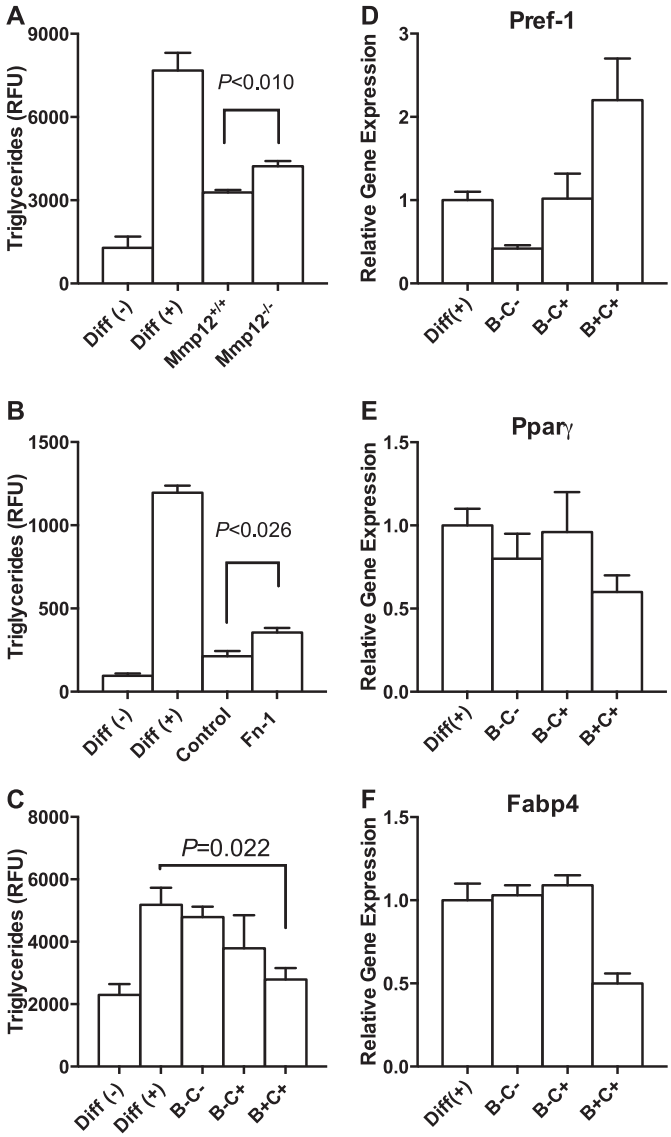

FIGURE 6. **Inhibition of adipocyte differentiation by $CD45^+CD11b^+$ $CD11c^+$ myeloid cells.** *A*, increased adipogenesis in preadipocytes treated with BM-DC-conditioned medium from $Mmp12^{-/-}$ mice. *B*, increased adipogenesis in preadipocytes treated with conditioned medium from BM-DCs in which Fn1 had been silenced. Both experiments were repeated four times, and representative experiments are presented. *C*, inhibition of adipogenesis when preadipocytes are co-cultured with $CD45^+CD11b^+CD11c^+$ cells. The experiment was repeated three times. *D–F*, panel of adipogenesis genes for the $CD45^+CD11b^+CD11c^+$ co-culture experiments.

that bold phenotypic changes are observed when lean mice receive a low fat diet. Therefore, the $Csf2^{-/-}$ mouse appears to be a unique model for understanding the relationships among adipose tissue expansion, immunity, and glucose homeostasis. Further work is required to understand whether the contribution of DCs to glucose homeostasis is a direct effect or the result of adipose tissue expansion.

Adipose Tissue DCs, but Not Macrophages, Suppress Adipose Tissue Expansion and Adipogenesis—Monocytes continuously enter peripheral tissues, where they can differentiate into DCs in the presence of GM-CSF (45, 46). DC differentiation also occurs during trans-endothelial monocyte trafficking (46). A tissue's content of DCs is maintained in a steady state at sites of potential pathogen entry, where these cells patrol the environ-

ment for invading pathogens. However, our work strongly suggests a novel function for resident white adipose tissue DCs: controlling normal adipose tissue development and adipogenesis to prevent uncontrolled expansion of the tissue.

White adipose tissue cannot be detected macroscopically during embryonic development in rodents, but it becomes visible 2–3 weeks after birth (47), when the *Csf2*$^{-/-}$ adipose tissue phenotype also becomes detectable. We show that white adipose tissue CD45^{+}CD11b^{+}Cd11c^{+} DCs are markedly reduced in very young *Csf2*$^{-/-}$ mice (3–4 weeks of age) and that low levels are maintained in adult (25 weeks of age) mice. Loss of adipose tissue DCs is associated with a clear increase in white adipose tissue mass and adipocyte cell size. Furthermore, we show that DCs isolated from adipose tissue have the ability to suppress adipocyte TG accumulation, most likely by secreting certain proteins. Together, our data provide strong evidence that white adipose tissue DCs suppress adipose tissue expansion.

There were clear differences between the abilities of DCs and macrophages to suppress adipogenesis. Medium conditioned by BM-DMs had no effect on adipogenesis *in vitro*, whereas medium conditioned by BM-DCs was dramatically inhibitory. We obtained similar results when we compared CD45^{+}CD11b^{+} Cd11c^{+} DCs with non-DC populations isolated from adipose tissue.

Although conditioned medium from macrophage cell lines was previously shown to inhibit adipocyte differentiation (48–50), the physiological relevance of those cell lines is unclear, and we were unable to repeat these results with bone marrow-derived macrophage-conditioned medium. Furthermore, the previous studies did not establish a concentration-dependent effect of macrophage-conditioned media on adipocyte differentiation. Our thorough study examined the effect of several myeloid-derived populations on adipogenesis under physiological conditions by using *in vitro* models, *in vivo* isolated cells, and knock-out animal models.

In the lean state, there are very few (~1% of CD45^{+} cells) resident macrophages (CD45^{+}CD11b^{+}CD11c^{+}F4/80^{+}MHCI-I^{low}) in adipose tissue. Although they could play a role in adipogenesis, such a small population might have too small an effect to remodel adipose tissue *in vivo*.

Adipose Tissue DCs Secrete Proteins, Including MMP12 and Fibronectin, That Directly Suppress Adipocyte TG Accumulation—This study shows that adipose tissue DCs probably suppress adipogenesis by releasing inhibitory proteins. Mass spectrometric analysis of the secretome of DCs combined with gene knock-out and gene silencing experiments identified MMP12 and fibronectin as two such secreted proteins. Both can remodel the extracellular matrix, as required for adipogenesis. However, they accounted only modestly (though significantly) for the inhibitory effects of DCs on adipogenesis. Moreover, their absence did not fully reverse the inhibition of adipogenesis induced by DC-conditioned medium. This suggests that additional factors secreted from DCs help keep adipogenesis and adipose tissue expansion in check.

Although lack of MMP12 improved adipogenesis by only 30%, the involvement of this enzyme in adipose tissue regulation is consistent with observations of *Mmp12*$^{-/-}$ mice, which are prone to obesity (26). This phenotype suggests that MMP12 helps suppress adipose tissue expansion and that adipose tissue DCs could be a major source of that enzyme.

Other studies support the concept that Pref-1 and fibronectin inhibit preadipocyte differentiation *in vitro* (8). For example, Pref-1 is highly expressed by preadipocytes. Moreover, treating preadipocytes with soluble Pref-1 inhibits adipogenesis by activating the MEK/ERK pathway (51, 52). Adiposity increases in Pref-1 knock-out mice, as does adipogenesis (39). It was recently shown that Pref-1 exerts its inhibitory function by binding to the C-terminal region of fibronectin, which in turn activates the MEK/ERK pathway (8, 52). Thus, the interaction of fibronectin with Pref-1 could inhibit adipogenesis directly. However, treating human preadipocytes with either macrophage- or monocyte-conditioned media decreased fibronectin levels in preadipocytes and increased collagen I and III levels (49). Therefore, it is possible that fibronectin inhibits adipogenesis indirectly by modulating the extracellular matrix. However, we did not detect significant changes in Itgam and Itg2 expression levels in wild type or *Csf2*$^{-/-}$ adipose tissue, although fibronectin has been shown to interact with integrins to form extracellular matrix (53). Thus, further work is required to determine how fibronectin secreted from DCs can suppress adipogenesis and extracellular matrix and participate in adipose tissue remodeling.

In addition to the factors we identified, other proteins are likely to inhibit adipogenesis and adipose tissue expansion by forming a coordinated network that prevents unwanted adipogenesis. For example, TNF-α, which is also secreted by BM-DCs, was shown to inhibit adipogenesis in 3T3-L1 cells via a β-catenin/TCF4-dependent pathway (54).

In summary, our observations demonstrate that DCs play an important role in white adipose tissue because they suppress adipogenesis and adipose tissue expansion. We also determined that fibronectin and MMP12, which are secreted from DCs, contribute to that inhibition.

References

1. Nishimura, S., Manabe, I., Nagasaki, M., Hosoya, Y., Yamashita, H., Fujita, H., Ohsugi, M., Tobe, K., Kadowaki, T., Nagai, R., and Sugiura, S. (2007) Adipogenesis in obesity requires close interplay between differentiating adipocytes, stromal cells, and blood vessels. *Diabetes* **56,** 1517–1526
2. Rosen, E. D., and Spiegelman, B. M. (2006) Adipocytes as regulators of energy balance and glucose homeostasis. *Nature* **444,** 847–853
3. Rosenson, R. S., Brewer, H. B., Jr., Chapman, M. J., Fazio, S., Hussain, M. M., Kontush, A., Krauss, R. M., Otvos, J. D., Remaley, A. T., and Schaefer, E. J. (2011) HDL measures, particle heterogeneity, proposed nomenclature, and relation to atherosclerotic cardiovascular events. *Clin. Chem.* **57,** 392–410
4. Morrison, R. F., and Farmer, S. R. (2000) Hormonal signaling and transcriptional control of adipocyte differentiation. *J. Nutr.* **130,** 3116S–3121S
5. O'Connell, J., Lynch, L., Hogan, A., Cawood, T. J., and O'Shea, D. (2011) Preadipocyte factor-1 is associated with metabolic profile in severe obesity. *J. Clin. Endocrinol. Metab.* **96,** E680–E684
6. Sul, H. S. (2009) Minireview: Pref-1: role in adipogenesis and mesenchymal cell fate. *Mol. Endocrinol.* **23,** 1717–1725
7. Lee, K., Villena, J. A., Moon, Y. S., Kim, K.-H., Lee, S., Kang, C., and Sul, H. S. (2003) Inhibition of adipogenesis and development of glucose intolerance by soluble preadipocyte factor-1 (Pref-1). *J. Clin. Invest.* **111,** 453–461
8. Wang, Y., Hudak, C., and Sul, H. S. (2010) Role of preadipocyte factor 1 in adipocyte differentiation. *Clin. Lipidol.* **5,** 109–115

9. Banchereau, J., and Steinman, R. M. (1998) Dendritic cells and the control of immunity. *Nature* **392,** 245–252
10. Heath, W. R., and Carbone, F. R. (2009) Dendritic cell subsets in primary and secondary T cell responses at body surfaces. *Nat. Immunol.* **10,** 1237–1244
11. Helft, J., Ginhoux, F., Bogunovic, M., and Merad, M. (2010) Origin and functional heterogeneity of non-lymphoid tissue dendritic cells in mice. *Immunol. Rev.* **234,** 55–75
12. Hamilton, J. A. (2008) Colony-stimulating factors in inflammation and autoimmunity. *Nat. Rev. Immunol.* **8,** 533–544
13. van de Laar, L., Coffer, P. J., and Woltman, A. M. (2012) Regulation of dendritic cell development by GM-CSF: molecular control and implications for immune homeostasis and therapy. *Blood* **119,** 3383–3393
14. Lutz, M. B., Kukutsch, N., Ogilvie, A. L., Rössner, S., Koch, F., Romani, N., and Schuler, G. (1999) An advanced culture method for generating large quantities of highly pure dendritic cells from mouse bone marrow. *J. Immunol. Methods* **223,** 77–92
15. Inaba, K., Inaba, M., Romani, N., Aya, H., Deguchi, M., Ikehara, S., Muramatsu, S., and Steinman, R. M. (1992) Generation of large numbers of dendritic cells from mouse bone marrow cultures supplemented with granulocyte/macrophage colony-stimulating factor. *J. Exp. Med.* **176,** 1693–1702
16. Becker, L., Liu, N.-C., Averill, M. M., Yuan, W., Pamir, N., Peng, Y., Irwin, A. D., Fu, X., Bornfeldt, K. E., and Heinecke, J. W. (2012) Unique proteomic signatures distinguish macrophages and dendritic cells. *PLoS One* **7,** e33297
17. Mabbott, N. A., Kenneth Baillie, J., Hume, D. A., and Freeman, T. C. (2010) Meta-analysis of lineage-specific gene expression signatures in mouse leukocyte populations. *Immunobiology* **215,** 724–736
18. Zhu, S. N., Chen, M., Jongstra-Bilen, J., and Cybulsky, M. I. (2009) GM-CSF regulates intimal cell proliferation in nascent atherosclerotic lesions. *J. Exp. Med.* **206,** 2141–2149
19. Mystkowski, P., Shankland, E., Schreyer, S. A., LeBoeuf, R. C., Schwartz, R. S., Cummings, D. E., Kushmerick, M., and Schwartz, M. W. (2000) Validation of whole-body magnetic resonance spectroscopy as a tool to assess murine body composition. *Int. J. Obes. Relat. Metab. Disord.* **24,** 719–724
20. Pamir, N., McMillen, T. S., Edgel, K. A., Kim, F., and LeBoeuf, R. C. (2012) Deficiency of lymphotoxin-α does not exacerbate high-fat diet-induced obesity but does enhance inflammation in mice. *Am. J. Physiol. Endocrinol. Metab.* **302,** E961–E971
21. McLean, J. A., and Tobin, G. (1987) *Human and Animal Calorimetry*, pp. 52–54, Cambridge University Press, New York
22. Pamir, N., McMillen, T. S., Kaiyala, K. J., Schwartz, M. W., and LeBoeuf, R. C. (2009) Receptors for tumor necrosis factor-α play a protective role against obesity and alter adipose tissue macrophage status. *Endocrinology* **150,** 4124–4134
23. Soukas, A., Socci, N. D., Saatkamp, B. D., Novelli, S., and Friedman, J. M. (2001) Distinct transcriptional profiles of adipogenesis *in vivo* and *in vitro*. *J. Biol. Chem.* **276,** 34167–34174
24. Livak, K. J., and Schmittgen, T. D. (2001) Analysis of relative gene expression data using real-time quantitative PCR and the $2(-\Delta\Delta C(T))$ method. *Methods* **25,** 402–408
25. Ingraham, C. A., Park, G. C., Makarenkova, H. P., and Crossin, K. L. (2011) Matrix metalloproteinase (MMP)-9 induced by Wnt signaling increases the proliferation and migration of embryonic neural stem cells at low O_2 levels. *J. Biol. Chem.* **286,** 17649–17657
26. Lee, J.-T., Pamir, N., Liu, N.-C., Kirk, E. A., Averill, M. M., Becker, L., Larson, I., Hagman, D. K., Foster-Schubert, K. E., van Yserloo, B., Bornfeldt, K. E., LeBoeuf, R. C., Kratz, M., and Heinecke, J. W. (2014) Macrophage metalloelastase (MMP12) regulates adipose tissue expansion, insulin sensitivity, and expression of inducible nitric oxide synthase. *Endocrinology* **155,** 3409–3420
27. Peng, Y., and Elkon, K. B. (2011) Autoimmunity in MFG-E8-deficient mice is associated with altered trafficking and enhanced cross-presentation of apoptotic cell antigens. *J. Clin. Invest.* **121,** 2221–2241
28. Schreyer, S. A., Peschon, J. J., and LeBoeuf, R. C. (1996) Accelerated atherosclerosis in mice lacking tumor necrosis factor receptor p55. *J. Biol. Chem.* **271,** 26174–26178
29. Hamilton, J. A., Davis, J., Pobjoy, J., and Cook, A. D. (2012) GM-CSF is not essential for optimal fertility or for weight control. *Cytokine* **57,** 30–31
30. Kim, D.-H., Sandoval, D., Reed, J. A., Matter, E. K., Tolod, E. G., Woods, S. C., and Seeley, R. J. (2008) The role of GM-CSF in adipose tissue inflammation. *Am. J. Physiol. Endocrinol. Metab.* **295,** E1038–E1046
31. Kahn, B. B., and Flier, J. S. (2000) Obesity and insulin resistance. *J. Clin. Invest.* **106,** 473–481
32. Sun, K., Kusminski, C. M., and Scherer, P. E. (2011) Adipose tissue remodeling and obesity. *J. Clin. Invest.* **121,** 2094–2101
33. Kingston, D., Schmid, M. A., Onai, N., Obata-Onai, A., Baumjohann, D., and Manz, M. G. (2009) The concerted action of GM-CSF and Flt3-ligand on *in vivo* dendritic cell homeostasis. **114,** 835–843
34. Hume, D. A. (2008) Differentiation and heterogeneity in the mononuclear phagocyte system. *Mucosal Immunol.* **1,** 432–441
35. Cheong, C., Matos, I., Choi, J.-H., Dandamudi, D. B., Shrestha, E., Longhi, M. P., Jeffrey, K. L., Anthony, R. M., Kluger, C., Nchinda, G., Koh, H., Rodriguez, A., Idoyaga, J., Pack, M., Velinzon, K., Park, C. G., and Steinman, R. M. (2010) Microbial stimulation fully differentiates monocytes to DC-SIGN/CD209(+) dendritic cells for immune T cell areas. *Cell* **143,** 416–429
36. Merad, M., and Manz, M. G. (2009) Dendritic cell homeostasis. *Blood* **113,** 3418–3427
37. Serbina, N. V., Salazar-Mather, T. P., Biron, C. A., Kuziel, W. A., and Pamer, E. G. (2003) TNF/iNOS-producing dendritic cells mediate innate immune defense against bacterial infection. *Immunity* **19,** 59–70
38. de Jong, E. C., Smits, H. H., and Kapsenberg, M. L. (2005) Dendritic cell-mediated T cell polarization. *Springer Semin. Immunopathol.* **26,** 289–307
39. Moon, Y. S., Smas, C. M., Lee, K., and Villena, J. A. (2002) Mice lacking paternally expressed Pref-1/Dlk1 display growth retardation and accelerated adiposity. *Mol. Cell. Biol.* **22,** 5585–5592
40. Plenz, G., Eschert, H., Beissert, S., Arps, V., Sindermann, J. R., Robenek, H., and Völker, W. (2003) Alterations in the vascular extracellular matrix of granulocyte macrophage colony-stimulating factor (GM-CSF)-deficient mice. *FASEB J.* **17,** 1451–1457
41. Spiegelman, B. M., and Ginty, C. A. (1983) Fibronectin modulation of cell-shape and lipogenic gene-expression in 3t3-adipocytes. *Cell* **35,** 657–666
42. Averill, M. M., Kerkhoff, C., and Bornfeldt, K. E. (2012) S100A8 and S100A9 in cardiovascular biology and disease. *Arterioscler. Thromb. Vasc. Biol.* **32,** 223–229
43. Guyenet, S. J., and Schwartz, M. W. (2012) Clinical review: Regulation of food intake, energy balance, and body fat mass: implications for the pathogenesis and treatment of obesity. *J. Clin. Endocrinol. Metab.* **97,** 745–755
44. Virtue, S., and Vidal-Puig, A. (2008) It's not how fat you are, it's what you do with it that counts. *PLoS Biol.* **6,** e237
45. Gordon, S., and Taylor, P. R. (2005) Monocyte and macrophage heterogeneity. *Nat. Rev. Immunol.* **5,** 953–964
46. Randolph, G. J., Inaba, K., Robbiani, D. F., Steinman, R. M., and Muller, W. A. (1999) Differentiation of phagocytic monocytes into lymph node dendritic cells *in vivo*. *Immunity* **11,** 753–761
47. Ailhaud, G., Grimaldi, P., and Négrel, R. (1992) Cellular and molecular aspects of adipose tissue development. *Annu. Rev. Nutr.* **12,** 207–233
48. Lu, C., Kumar, P. A., Fan, Y., Sperling, M. A., and Menon, R. K. (2010) A novel effect of growth hormone on macrophage modulates macrophage-dependent adipocyte differentiation. *Endocrinology* **151,** 2189–2199
49. Gagnon, A., Yarmo, M. N., Landry, A., and Sorisky, A. (2012) Macrophages alter the differentiation-dependent decreases in fibronectin and collagen I/III protein levels in human preadipocytes. *Lipids* **47,** 873–880
50. Bilkovski, R., Schulte, D. M., Oberhauser, F., Mauer, J., Hampel, B., Gutschow, C., Krone, W., and Laudes, M. (2011) Adipose tissue macrophages inhibit adipogenesis of mesenchymal precursor cells via wnt-5a in humans. *Int. J. Obes.* (*Lond.*) **35,** 1450–1454
51. Mei, B., Zhao, L., Chen, L., and Sul, H. S. (2002) Only the large soluble form

of preadipocyte factor-1 (Pref-1), but not the small soluble and membrane forms, inhibits adipocyte differentiation: role of alternative splicing. *Biochem. J.* **364,** 137–144

52. Kim, K.-A., Kim, J.-H., Wang, Y., and Sul, H. S. (2007) Pref-1 (preadipocyte factor 1) activates the MEK/extracellular signal-regulated kinase pathway to inhibit adipocyte differentiation. *Mol. Cell. Biol.* **27,** 2294–2308
53. Aota, S., Nagai, T., Olden, K., Akiyama, S. K., and Yamada, K. M. (1991) (1991) Fibronectin and integrins in cell adhesion and migration. *Biochem. Soc. Trans.* **19,** 830–835
54. Cawthorn, W. P., Heyd, F., Hegyi, K., and Sethi, J. K. (2007) Tumour necrosis factor-α inhibits adipogenesis via a β-catenin/TCF4(TCF7L2)-dependent pathway. *Cell Death Differ.* **14,** 1361–1373